

Chapter 4

FORCED VIBRATION ANALYSIS OF PLATES - TRANSVERSE FORCE

1. INTRODUCTION

In Chapter 2, the mathematical model of the p-version of the FEM has been derived including geometrical non-linearity for thick, asymmetric laminated rectangular plates. In this chapter, only symmetrically laminated plates, i.e., $[B]=0$, made of composite materials are studied. Before applying the model to geometrically non-linear analysis, it is worth applying the model to linear free vibration analysis. The excitation used in the forced vibration is a harmonic plane wave. The convergence of the model developed is studied. Results are also presented for non-linear forced vibrations. Fully clamped symmetrically laminated rectangular plates are here analysed. A different number of in-plane and out-of-plane shape functions are considered and the obtained results are compared with numerical results from the literature.

The study of linear dynamic behaviour of plates is not a new topic. Leissa [4.1] gave an extensive study of plate vibration. Lin and Kin [4.2] used classical laminated plate theory to compute the natural frequencies of un-symmetrically laminated, rectangular plates. Reddy [4.3] developed a finite element method based on a typical first order laminated theory and computed the natural frequencies of simply supported, anti-symmetric angle-ply, laminated plates. Bert and Mayberry [4.4] predicted the natural frequencies of un-symmetrically laminated plates with clamped edges using Raleigh-Ritz energy method. Chow, Liew and Lam [4.5] investigated the free vibration of symmetrically laminated plates with the Raleigh-Ritz method using admissible 2-D orthogonal polynomials. Some experimental work on the dynamic response of

laminated plates under acoustic excitation was carried out in the Institute of Sound and Vibration Research at Southampton University [4.14].

One of the main applications of laminated composite plates is that of skin-panels in aircraft. These panels, especially those near the jet engine's exhaust, work under high level acoustic pressure environment combined with pressure due to service loads. In this work, the dynamic response of laminated composite plates excited by harmonic plane waves is investigated. The Newmark method presented in Chapter 2 is applied to solve the equations of motion.

In order to analyse the time domain response of the plate's vibrations, the tools presented in Chapter 3 are used to determine the presence of a periodic, quasi-periodic or chaotic motion.

2. PLATES ANALYSED

Three symmetric, rectangular graphite/epoxy composite laminated plates are considered, therefore, there is no bending-twisting stiffness, i.e., $[B]=0$. Their geometrical and material properties are defined in Table 1 and in Table 2. It was assumed that G_{13} and G_{23} are equal to G_{12} .

Table 1- Geometrical properties of the plates

Plate	Number of lamina	Laminae orientation	$a(m)$	$b(m)$	$h(m)$
1	8	$(90,-45,45,0)_{sym.}$	0.48	0.32	0.001
2	5	$(\theta,-\theta,\theta,-\theta,\theta)$	0.3	0.3	0.001
3	3	$(45,-45,45)$	0.5	0.5	0.005

Table 2 – Material properties of the plates

Plate	E_{11} (N/m^2)	E_{22} (N/m^2)	G_{12} (N/m^2)	ρ (Kgm^{-3})	ν_{12}
1	120.5×10^9	9.63×10^9	3.58×10^9	1540	0.32
2	173.0×10^9	E11/15.4	$0.79 \times E_{22}$	1540	0.3
3	206.84×10^9	5.171×10^9	2.5855×10^9	2564.856	0.25

The mode shapes of laminated composite rectangular plates depend not only upon the aspect ratio of the plates, but also on the elastic properties of the laminae and the orientations. For symmetrically laminated composite rectangular plates, the mode shape patterns are complicated by twisting-bending coupling. This coupling distorts the mode shapes of the plates. It is difficult to find a purely symmetric or antisymmetric mode in symmetrically laminated rectangular plates. Errors are inevitable if only symmetric or antisymmetric displacement functions are used in modelling a certain mode for this kind of plates.

3. LINEAR VIBRATION ANALYSIS

3.1 - Convergence with the number of shape functions

Consider a fully clamped rectangular carbon fibre reinforced symmetrically laminated plate. The plate displacement shape functions in the x and the y axes were defined in Chapter 2, as well as the rotations. These functions satisfy the fully clamped theoretical boundary conditions, i.e., zero displacement and zero slopes along the four plate edges; moreover they have been used and shown to be appropriate in previous studies on the vibration of fully clamped rectangular plates [4.8, 4.9, and 4.10]. The analytical expressions of the shape functions of the clamped-clamped plate are given in Chapter 2.

In this convergence study, a different number of in plane and out of plane shape functions are used in the model. In order to analyse the convergence of the linear frequencies, seven rotational shape functions are used in plates 1 and 3, and nine are considered in plate 2. The convergence of the model is assured comparing the values obtained for the natural frequencies, ω , with published results.

The influence of p_θ in the prediction of the linear frequencies is also considered, and the results are discussed for plate 1. In Tables 3 to 7, the convergence of the first four linear frequencies, ω_i , $i=1,2,3,4$, of the plates is studied:

Table 3- Natural frequencies of plate 1 with $p_i=p_\theta=7$

p_o	4	5	6	7	8	9	10	11
DOF	114	123	134	147	162	179	198	219
ω_1	511.149	511.112	511.111	511.105	511.104	511.101	511.101	511.100
ω_2	645.189	644.977	644.967	644.959	644.956	644.953	644.951	644.948
ω_3	902.541	886.334	886.328	886.310	886.308	886.300	886.299	886.294
ω_4	1313.790	1307.348	1301.312	1301.272	1301.198	1301.154	1301.140	1301.111

Table 4 - Natural frequencies of plate 2 with $p_i=p_\theta=7, \theta = 45^\circ$

p_o	4	5	6	7	8	9	10	11
DOF	114	123	134	147	162	179	198	219
ω_1	762.888	762.863	762.838	762.831	762.828	762.825	762.824	762.822
ω_2	1419.717	1419.674	1419.507	1419.505	1419.475	1419.474	1419.464	1419.463
ω_3	1647.676	1647.104	1646.861	1646.838	1646.809	1646.798	1646.789	1646.782
ω_4	2234.666	2219.137	2218.961	2218.928	2218.873	2218.860	2218.843	2218.835

Table 5 – Linear natural frequency parameter λ and linear frequencies of symmetrically five layer angle-ply ($\theta = 0^\circ$), square plate 2 with fully clamped edges, $p_i=p_\theta=9$, $\left(\lambda = (\rho h \omega^2 a^4 / D_0)^{1/2} \right)$,

$$D_0 = \frac{E_{11} h^3}{12(1 - \nu_{12} \nu_{21})}, \text{ (Graphite/Epoxy, } E_{11} / E_{22} = 15.4, G_{12} / E_{22} = 0.79, \nu_{12} = 0.30)$$

p_o	4		5		6		7	
λ / ω	λ_i	ω_i	λ_i	ω_i	λ_i	ω_i	λ_i	ω_i
	23.840	812.856	23.839	812.819	23.839	812.819	23.839	812.816
	29.705	1012.815	29.704	1012.797	29.701	1012.677	29.700	1012.677
	42.813	1459.733	41.744	1423.701	41.744	1423.301	41.704	1421.928
	62.924	2145.456	62.922	2145.369	60.202	2052.649	60.202	2052.649
	64.563	2201.322	64.562	2201.293	62.900	2144.633	62.900	2144.627
p_o	8		9		10		11	
λ / ω	λ_i	ω_i	λ_i	ω_i	λ_i	ω_i	λ_i	ω_i
	23.839	812.816	23.839	812.811	23.839	812.811	23.839	812.809
	29.700	1012.677	29.700	1012.672	29.700	1012.671	29.700	102.668
	41.704	1421.928	41.703	1421.920	41.703	1421.920	41.703	1421.916
	60.146	2050.720	60.145	2050.711	60.145	2050.711	60.144	2050.674
	62.900	2144.627	62.900	2144.626	62.899	2144.603	62.899	2144.603

Table 6 - Natural frequencies of plate 3 with $p_i = p_\theta = 7$

p_o	4	5	6	7	8	9	10	11
DOF	114	123	134	147	162	179	198	219
ω_1	954.792	952.956	952.610	952.478	952.377	952.321	952.270	952.236
ω_2	1558.468	1557.922	1557.105	1556.940	1556.650	1556.603	1556.429	1556.402
ω_3	2234.674	2203.451	2196.995	2196.100	2195.495	2195.155	2194.925	2194.925
ω_4	2318.568	2273.654	2270.775	2269.591	2269.494	2268.938	2268.906	2268.572

From Tables 3 to 6, the convergence of the first four linear frequencies is assured for all the plates studied. In order to validate the model, in Tables 7, 8 and 9, the results obtained with the first order shear deformation model for thick plates, are compared with results obtained with the HFEM from the thin plate theory.

Table 7- Convergence of the first four linear frequencies (rad/s) of Plate 1, with the number of out of plane shape functions

* - Thin Plate theory ** - First Order Shear Deformation Theory for thick plates

Mode	[4.9]*	FSDT**					
	$p_o=7, 49$ DOF	$p_o=5, p_i=7, p_o=6, p_i=7, p_o=7, p_i=7, p_o=8, p_i=7, p_o=8, p_i=8,$ $p_\theta=7, n=123$	$p_\theta=7,$ $n=134$	$p_\theta=7,$ $n=147$	$p_\theta=7,$ $n=162$	$p_\theta=8,$ $n=192$	$p_o=8, p_i=9,$ $p_\theta=9, n=226$
1	511.390	511.112	511.111	511.105	511.104	511.091	511.087
2	645.281	644.977	644.967	644.959	644.956	644.895	644.881
3	886.217	886.334	886.328	886.310	886.308	886.167	885.628
4	-	1307.348	1301.312	1301.272	1301.198	1236.386	1235.338

Table 8 - Convergence of the first four linear frequencies (rad/s) of Plate 2, $\theta = 45^\circ$, with $p_i = p_\theta = 7$ and the number of out of plane shape functions

Mode	[4.10]	FSDT		
	$p_o=7, 64$ DOF	$p_o=4, p_i=7,$ $p_\theta=7, n=114$	$p_o=5, p_i=7,$ $p_\theta=7, n=123$	$p_o=6, p_i=7,$ $p_\theta=7, n=134$
1	763.0961	762.888	762.863	762.838
2	1419.927	1419.717	1419.674	1419.507
3	1647.361	1647.676	1647.104	1646.861
4	2219.133	2234.666	2219.137	2218.961

It can be seen from the two Tables that the linear frequencies for p_o differ very slightly. Increasing p_o , the linear frequency, decreases monotonically towards a certain value, i.e., the errors between them decrease with the increase of p_o . Excellent convergence properties of the HFEM in the linear frequency analysis of symmetrically laminated plates are observed.

Table 7 and 8, the linear frequencies are lower than those obtained in [4.9, 4.10]. Although more shape functions are used, with 192 DOF for plate 1, and 134 DOF for plate 2, the thick plate theory gives better approximations than the thin plate theory where the rotatory inertia and shear deformation are neglected.

Table 9 - Convergence of the first four linear frequencies (rad/s) of Plate 3, with $p_i = p_\theta = 7$ and the number of out of plane shape functions

Mode	[4.11]	FSDT		
	$p_o=6, 36$ DOF	$p_o=4, p_i=7, p_\theta=7, n=114$	$p_o=5, p_i=7, p_\theta=7, n=123$	$p_o=6, p_i=7, p_\theta=7, n=134$
1	1574.96	954.792	952.956	952.610
2	2577.55	1558.468	1557.922	1557.105
3	3671.02	2234.674	2203.451	2196.995
4	-	2318.568	2273.654	2270.775

Possible reasons for the large differences encountered in

Table 9 are not only the different theories employed, but also the material properties assumed here for G_{13} and G_{23} , shear moduli which are not necessary in [4.11].

In Tables 7, 8 and 9, the element defined can determine correctly the first four linear frequencies of thin plates.

3.2 - The effect of b/h in the linear frequencies

In Tables 10, 11 and 12 the thickness of plate 1, 2 and 3 is changed and the convergence of the first four linear frequencies, $\omega_i, i=1,2,3,4$, of the plates is studied.

Table 10- Variation of the linear frequencies of vibration /different thickness of plate 1 with 134 DOF

ω_i	ω_1	ω_2	ω_3	ω_4
Model				
$b/h= 10000$	7.816	14.249	16.954	23.060
$b/h= 1000$	163.640	206.504	283.790	418.477
$b/h = 100$	1626.940	2052.411	2819.598	4045.113
$b/h = 10$	11205.824	14284.606	19578.063	23055.506

Table 11- Variation of the linear frequencies of vibration /different thickness of plate 2, $\theta = 45^\circ$, with 134 DOF

ω_i	ω_1	ω_2	ω_3	ω_4
Model				
$b/h= 1000$	228.939	426.110	494.431	666.204
$b/h = 100$	2281.255	4238.556	4912.275	6614.088
$b/h = 10$	18111.411	31179.616	34244.400	44915.726

Table 12- Variation of the linear frequencies of vibration /different thickness of plate 3 with 134 DOF

w_i	ω_1	ω_2	ω_3	ω_4
Model				
$b/h= 1000$	96.557	158.203	225.939	231.694
$b/h = 100$	952.610	1557.105	2196.995	2270.775
$b/h = 10$	5557.992	8642.435	10187.659	12030.861

From the three tables above, for thin ($b/h=1000$) and moderately thick ($b/h=100$) plates, the linear frequencies obtained are smaller than those of thick ($b/h=10$) plates, as expected.

3.3 - Influence of the fibre orientation in the prediction of the linear frequencies

In this section, a fibre orientation study is carried out for plate 2. In Table 13, the results for 7 out-of-plane and 9 rotational shape functions are presented and compared with published results.

Table 13 – Linear natural frequency parameter λ of symmetrically five layer angle-ply, square plate 2 with fully clamped edges and different angle orientation

θ	Mode	1	2	3	4
	Method				
0°	FSDT	23.839	29.700	41.704	60.202
0°	CPT [4.14] [4.15]	23.852	29.715	41.721	60.229
30°	FSDT	22.704	36.526	53.967	57.118
30°	CPT [4.14]	22.713	36.546	54.012	57.156
45°	FSDT	22.372	41.621	48.282	65.032
45°	CPT [4.14]	22.381	41.645	48.316	65.086

Outstanding agreement for all the three groups of results with three different angles θ , can be clearly seen in this table. In all the cases, the frequency parameters given by the first order shear deformation model are smaller than those given in [4.14] and [4.15]. It may be due to the inclusion of in-plane displacements and transverse shear deformation in the model developed in this thesis, which could slightly reduce the stiffening effects caused by neglecting these factors.

4. NON-LINEAR FORCED VIBRATION ANALYSIS

4.1 - Introduction

In this section, the discussion of forced vibration of a rectangular plate is studied using the HFEM, and equation (2.71) is solved by the Newmark method. If a distributed force that impinges on the plate's surface only in the z direction is

considered, then $\{P_u\} = \{P_v\} = 0$ and the new force vector is given by equation (2.78).

In non-linear vibrations, there are several parameters that influence the time dependence of the response: time variation, space dependence and amplitude of the external excitation, properties of the structure, initial and boundary conditions, etc. Depending on these parameters, the oscillations may be periodic – including harmonic, sub-harmonic and super-harmonic – quasi-periodic or even chaotic [4.12]. Quasi-periodic motion has a finite number of frequency components where some of them are not related by a rational number; therefore, its time signal is non-repetitive. A chaotic signal is as well non-repetitive in the time domain and has a very wide frequency spectrum.

For various amplitudes and frequencies of excitation, time domain simulations of the response of the plates were carried out. A *FORTRAN* [4.13] Newmark integration routine was used.

Applying the principle of the virtual work, the generalised external forces in the transverse direction were obtained in Chapter 2. It is recalled that for a distributed transverse force in the z direction one has the following expression:

$$\{P\} = \int_{\Omega} \{N^w\} P_d(x, y, t) d\Omega \quad (4.1)$$

where $\{N^w\}$ is the out of plane shape function vector. If a harmonic plane wave impinges on the plate's surface in the normal direction then

$$P_d(x, y, t) = F \cos(\omega t - k), k \in \mathbb{R} \quad (4.2)$$

where F is the magnitude of the applied force, ω is the frequency of the harmonic wave and k is the phase. Substituting (4.2) in (4.1), we have

$$\begin{aligned} \{P\} &= F \int_{\Omega} \{N^w\} d\Omega \cos(\omega t - k) \\ &= \{\bar{f}\} \cos(\omega t - k) \end{aligned} \quad (4.3)$$

The generalised external force vector $\{\bar{f}\}$ has only a real part in the above equation.

It is interesting to note that most of the components in $\{\bar{f}\}$ are zero. For a plate with fully clamped edges in which only the shape functions generated by equation (2.96) are used, only $\bar{f}(1)$ is different from zero. In this situation

$$\bar{f}(1) = F \frac{ab}{4} \int_{-1}^1 f_4(\xi) d\xi \int_{-1}^1 f_4(\eta) d\eta \quad (4.4)$$

in which, a and b are the in-plane dimensions of the plate, $f_4(\xi)$ and $f_4(\eta)$ are the first shape functions generated using equation (2.96).

4.2 - Numerical results

Plate 2 is excited by a harmonic wave of 4 N/m^2 and 123 DOF ($p_i=7, p_o=5, p_\theta=7$) are considered in the model. The fibres orientation varies from $\theta = 0^\circ$ to $\theta = 45^\circ$. The force applied to the plate is increased to 3000 N/m^2 for $\theta = 30^\circ$ and $\theta = 45^\circ$; for $\theta = 0^\circ$ it is increased to 3300 N/m^2 , and the results are discussed. For amplitudes of vibration of the order of the thickness of the plate, the solution was always periodic and highly dominated by the harmonic with frequency equal to the excitation frequency (principal harmonic).

Plate 1 is excited by a harmonic wave of 5 N/m^2 , and 123 DOF are considered. The force applied to the plate is increased to 3000 N/m^2 , at 511.112 rad/s . The results obtained are also discussed.

In Figure 1, the time domain response of the plate 2, $\theta = 45^\circ$ is presented for different values of α . Figure 2, shows that a closed path is obtained in the phase plane, therefore, the motion is periodic.

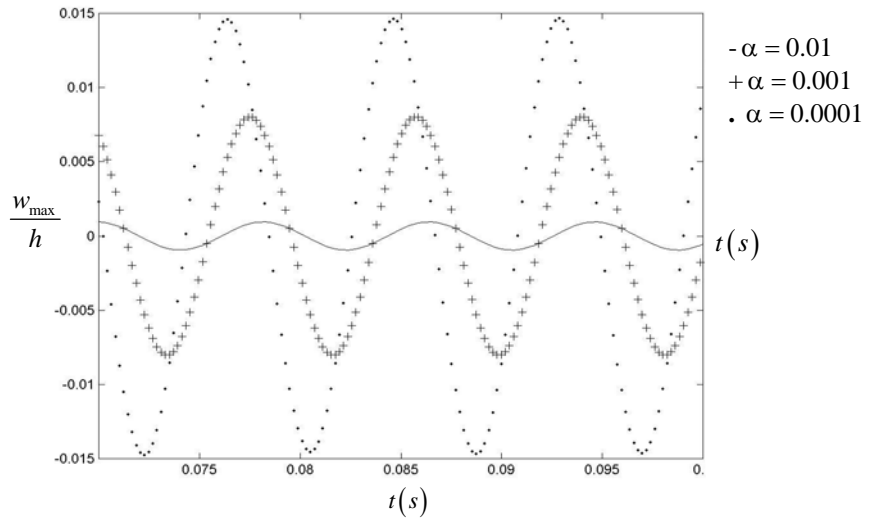


Figure 1 – Time domain response of Plate 2, (45, -45, 45, -45, 45) due to harmonic excitation by a plane wave of 4 N/m²

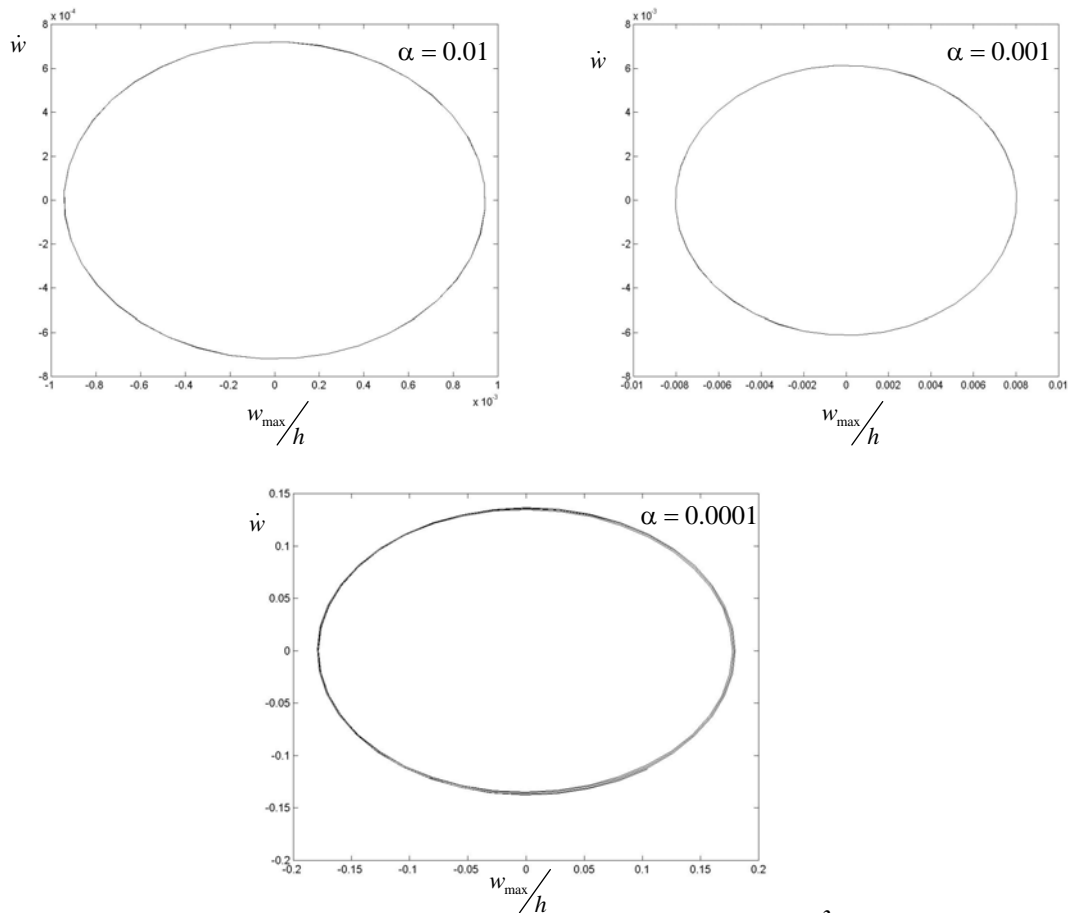


Figure 2 – Phase plane of the steady state forced vibration (4 N/m²) of Plate 2, (45, -45, 45, -45, 45) with different values of α

Considering these responses, the influence of the loss parameter in the vibration of plate 2 is investigated. In Figure 1, with $\alpha = 0.01$, the amplitude calculated at or near a point where it attains its maximum, w_{\max}/h , is given by 0.000941; with $\alpha = 0.001$, the value of w_{\max}/h is 0.00801, and when $\alpha = 0.0001$, w_{\max}/h is 0.01466. Therefore, diminishing the value of α implies an increase in the amplitude of vibration, as expected. In the following, α is 0.0001.

For plate 2, $\theta = 45^\circ$, and for plate 1, the Fourier spectra of the periodic responses due to a harmonic wave of 4 and 5 N/m^2 are defined. In Figures 3 and 4, the spectrum of the Fourier series of the plates excited at the first mode of vibration is presented. Once the spectrum consists of a single basic frequency, a periodic motion is achieved. The near absence of harmonics indicates that the plate is practically in the linear regime, which is a result of the small amplitudes of oscillation.

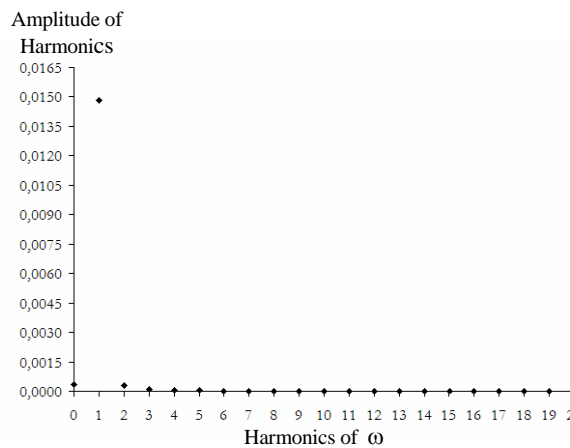


Figure 3 – Fourier spectrum of forced vibration of plate 2, (45,-45, 45,-45, 45) due to and harmonic excitation by a plane wave of 4 N/m^2

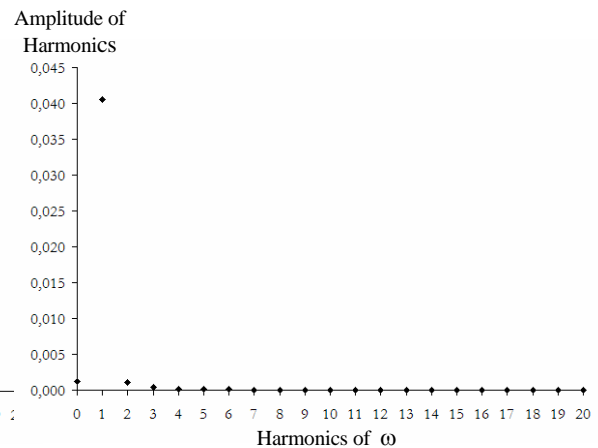


Figure 4 - Fourier spectrum of forced vibration of plate1, due to and harmonic excitation by a plane wave of 5 N/m^2

In Figures 5-16 the distributed force applied to plate 2 is increased; the response and the phase planes are presented.

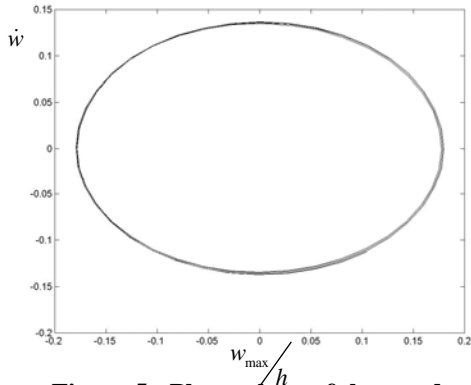


Figure 5 - Phase plane of the steady state forced vibration (50 N/m^2) of plate 2, (45,-45,45,-45,45) due to harmonic excitation by a plane wave

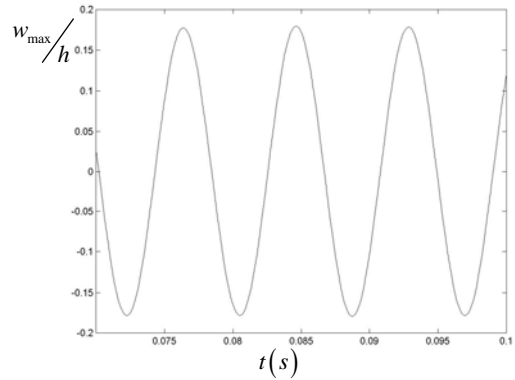


Figure 6 - Time domain response of Plate 2, (45,-45,45,-45,45) due to harmonic excitation by a plane wave of 50 N/m^2

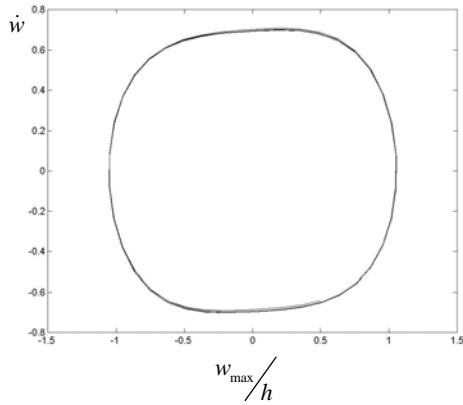


Figure 7 - Phase plane of the steady state forced vibration (500 N/m^2) of plate 2, (45,-45,45,-45,45) due to harmonic excitation by a plane wave

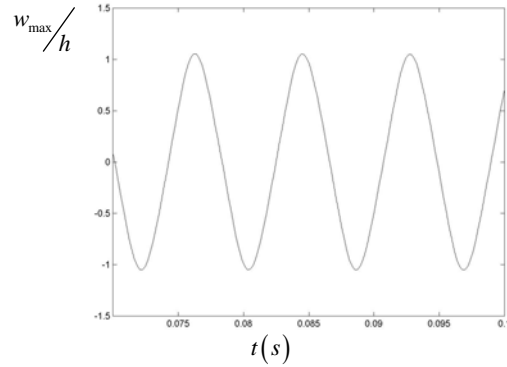


Figure 8 - Time domain response of Plate 2, (45,-45,45,-45,45) due to harmonic excitation by a plane wave of 500 N/m^2

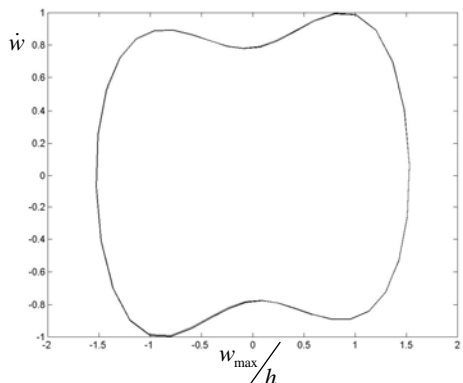


Figure 9 - Phase plane of the steady state forced vibration (1000 N/m^2) of plate 2, (45,-45,45,-45,45) due to harmonic excitation by a plane wave

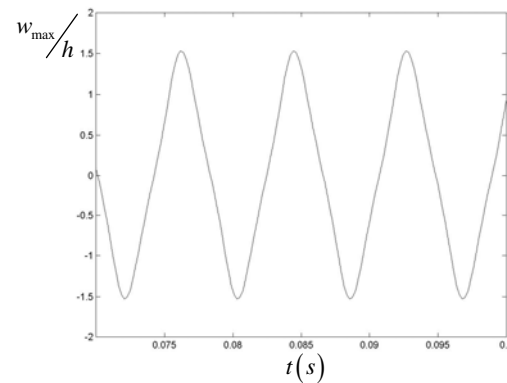


Figure 10 - Time domain response of Plate 2, (45,-45,45,-45,45) due to harmonic excitation by a plane wave of 1000 N/m^2

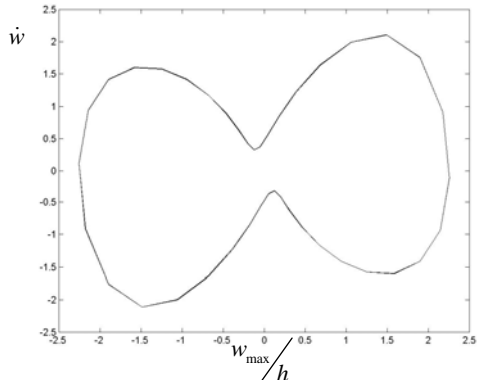


Figure 11 - Phase plane of the steady state forced vibration (2000 N/m^2) of plate 2, (45,-45,45,-45,45) due to harmonic excitation by a plane wave

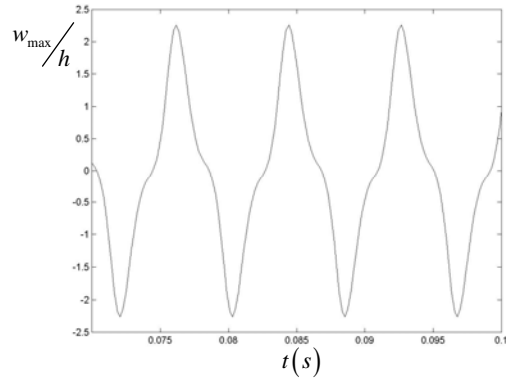


Figure 12 - Time domain response of Plate 2, (45,-45,45,-45,45) due to harmonic excitation by a plane wave of 2000 N/m^2

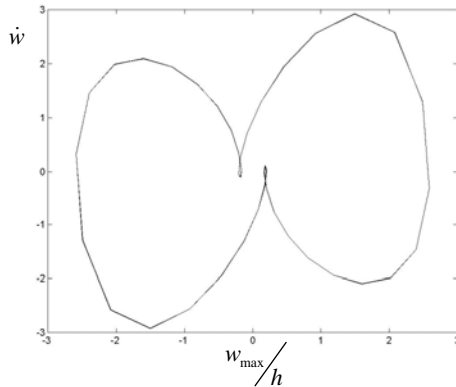


Figure 13 - Phase plane of the steady state forced vibration (2500 N/m^2) of plate 2, (45,-45,45,-45,45) due to harmonic excitation by a plane wave

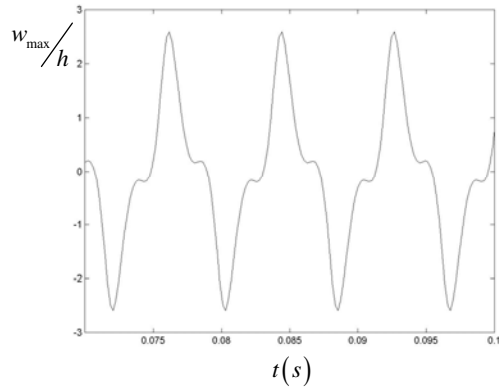


Figure 14 - Time domain response of Plate 2, (45,-45,45,-45,45) due to harmonic excitation by a plane wave of 2500 N/m^2

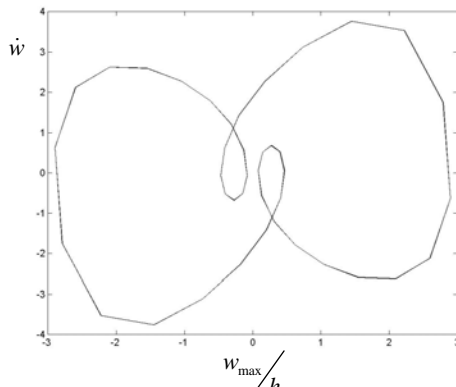


Figure 15 - Phase plane of the steady state forced vibration (3000 N/m^2) of plate 2, (45,-45,45,-45,45) due to harmonic excitation by a plane wave

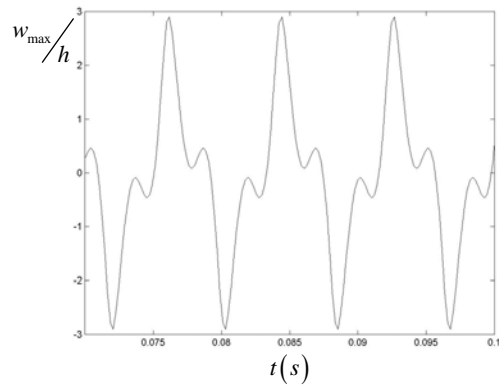


Figure 16 - Time domain response of Plate 2, (45,-45,45,-45,45) due to harmonic excitation by a plane wave of 3000 N/m^2

Closed paths are obtained in the phase planes for all the forces applied, therefore periodic motions are achieved. The values of w_{\max}/h are presented in Table 14, where P_d represents the distributed applied force.

Table 14 – Forced Vibration, Plate 2, $\theta = 45^\circ$, $p_0=5$

P_d (N/m^2)	$P_d = 4$	$P_d = 50$	$P_d = 500$	$P_d = 1000$	$P_d = 2000$	$P_d = 2500$	$P_d = 3000$
ω/ω_{l1}	w_{\max}/h						
1.0005	0.0147	0.1797	1.0536	1.5300	2.2628	2.5889	2.8998

The amplitude of vibration, w_{\max}/h , increases as the force applied to the plate increases, but the relation between them is not linear. Considering plate 2 with $\theta = 30^\circ$, the phase planes and the time domain responses for a force varying from $4 N/m^2$ to $3000 N/m^2$ are given by

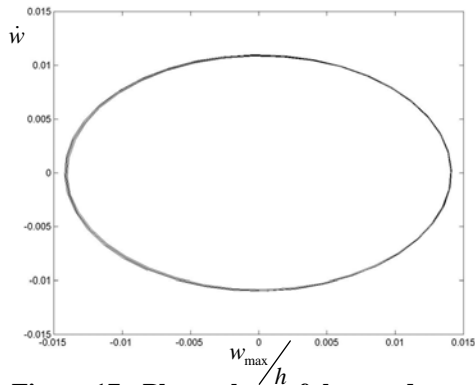


Figure 17 - Phase plane of the steady state forced vibration ($4N/m^2$) of plate 2, (30,- 30, 30,- 30, 30) due to harmonic excitation by a plane wave

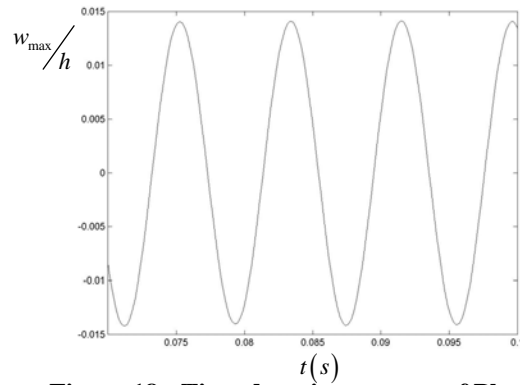


Figure 18 - Time domain response of Plate 2, (30,- 30, 30,- 30, 30) due to harmonic excitation by a plane wave of $4 N/m^2$

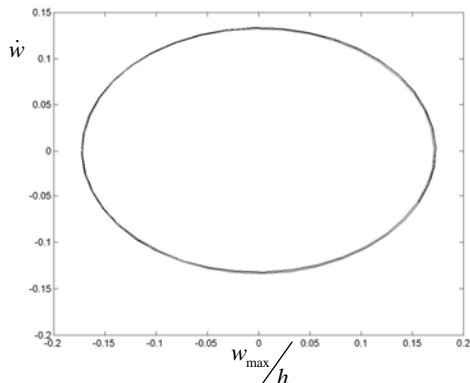


Figure 19 - Phase plane of the steady state forced vibration ($50N/m^2$) of plate 2, (30,- 30, 30,- 30, 30) due to harmonic excitation by a plane wave

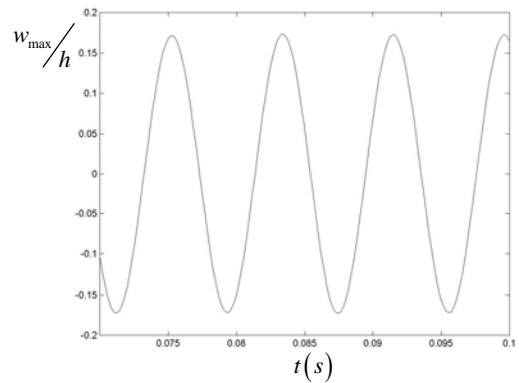


Figure 20 - Time domain response of Plate 2, (30,- 30, 30,- 30, 30) due to harmonic excitation by a plane wave of $50 N/m^2$

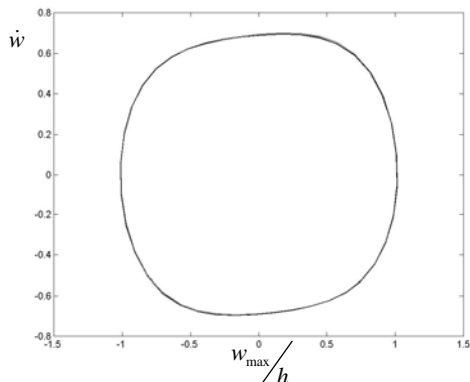


Figure 21 - Phase plane of the steady state forced vibration ($500N/m^2$) of plate 2, (30,- 30, 30,- 30, 30) due to harmonic excitation by a plane wave

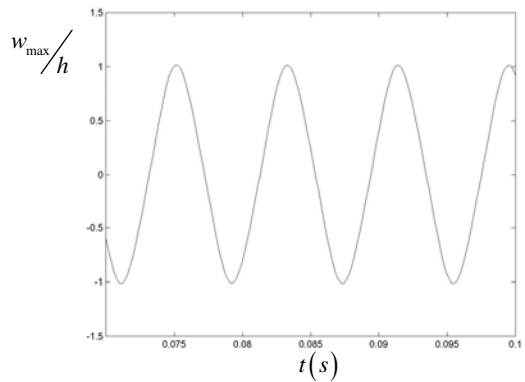


Figure 22 - Time domain response of Plate 2, (30,- 30, 30,- 30, 30) due to harmonic excitation by a plane wave of $500 N/m^2$

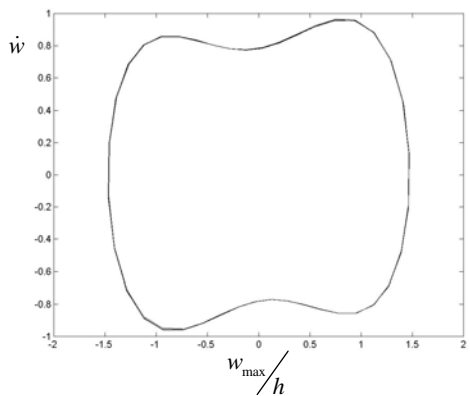


Figure 23 - Phase plane of the steady state forced vibration ($1000N/m^2$) of plate 2, (30,- 30, 30,- 30, 30) due to harmonic excitation by a plane wave

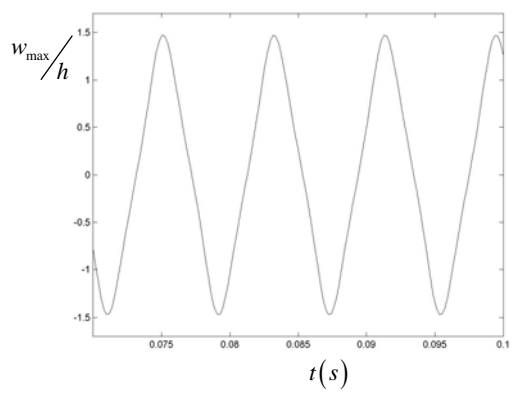


Figure 24 - Time domain response of Plate 2, (30,- 30, 30,- 30, 30) due to harmonic excitation by a plane wave of $1000 N/m^2$

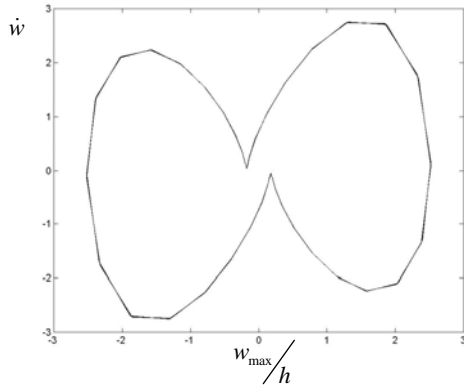


Figure 25 - Phase plane of the steady state forced vibration (2500N/m^2) of plate 2, (30,- 30, 30,- 30, 30) due to harmonic excitation by a plane wave

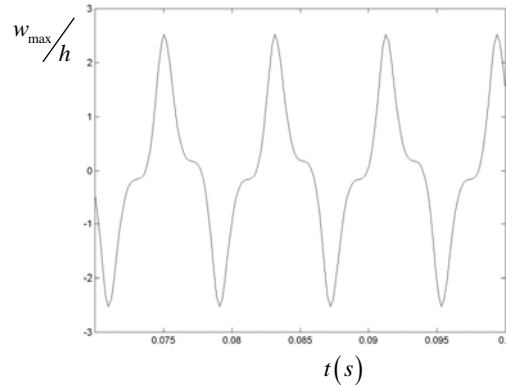


Figure 26 - Time domain response of Plate 2, (30,- 30, 30,- 30, 30) due to harmonic excitation by a plane wave of 2500 N/m^2

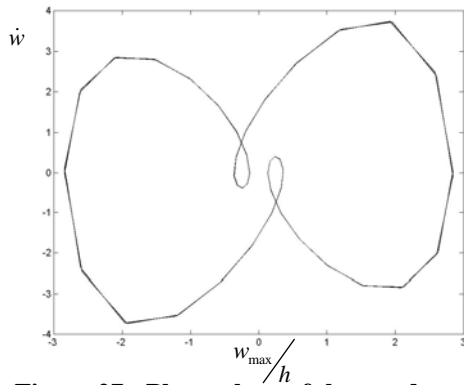


Figure 27 - Phase plane of the steady state forced vibration (3000N/m^2) of plate 2, (30,- 30, 30,- 30, 30) due to harmonic excitation by a plane wave

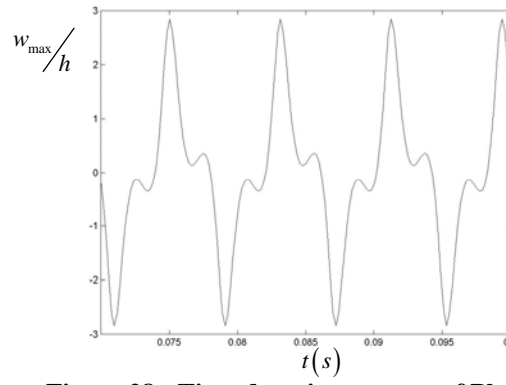


Figure 28 - Time domain response of Plate 2, (30,- 30, 30,- 30, 30) due to harmonic excitation by a plane wave of 3000 N/m^2

The amplitudes of vibration of plate 2, with $\theta = 30^\circ$ and for different distributed forces considered are presented in Table 15 and it can be seen that the amplitude of vibration increases as the force increases.

Table 15 - Forced Vibration, Plate 2, $\theta = 30^\circ$, $p_0=5$

P_d (N/m^2)	$P_d = 4$	$P_d = 50$	$P_d = 500$	$P_d = 1000$	$P_d = 2500$	$P_d = 3000$
ω / ω_{11}	w_{max} / h					
1.0004	0.0141	0.1732	1.0147	1.4739	2.5232	2.8444

Comparing with the results obtained in Table 14, for $\theta = 30^\circ$ the amplitudes of vibration are lower than those obtained for $\theta = 45^\circ$.

Finally, the results obtained for plate 2 with $\theta = 0^\circ$ are given by:

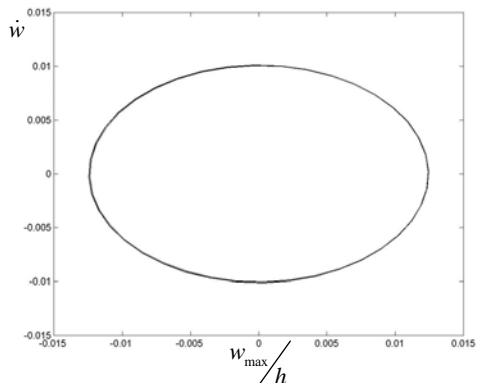


Figure 29 - Phase plane of the steady state forced vibration ($4 N/m^2$) of plate 2, (0,-0, 0, -0,0), due to harmonic excitation by a plane wave

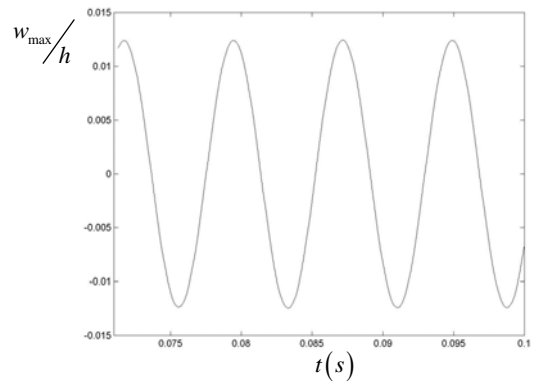


Figure 30 - Time domain response of Plate 2, (0,-0, 0, -0,0), due to harmonic excitation by a plane wave of $4 N/m^2$

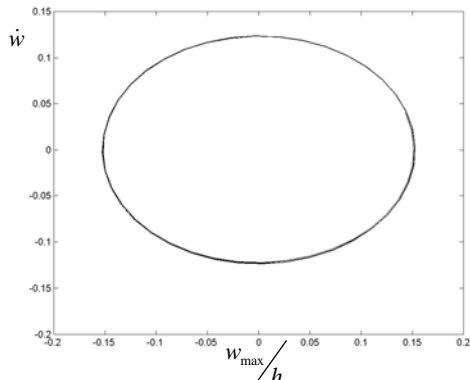


Figure 31 - Phase plane of the steady state forced vibration ($50 N/m^2$) of plate 2, (0,-0, 0, -0,0), due to harmonic excitation by a plane wave

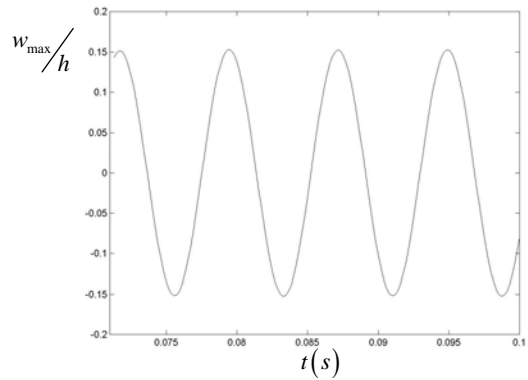


Figure 32 - Time domain response of Plate 2, (0,-0, 0, -0,0), due to harmonic excitation by a plane wave of $50 N/m^2$

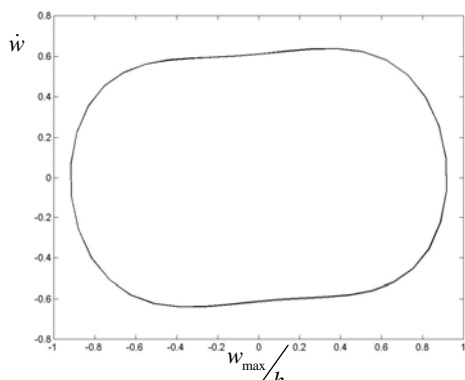


Figure 33 - Phase plane of the steady state forced vibration ($500 N/m^2$) of plate 2, (0,-0, 0, -0,0), due to harmonic excitation by a plane wave

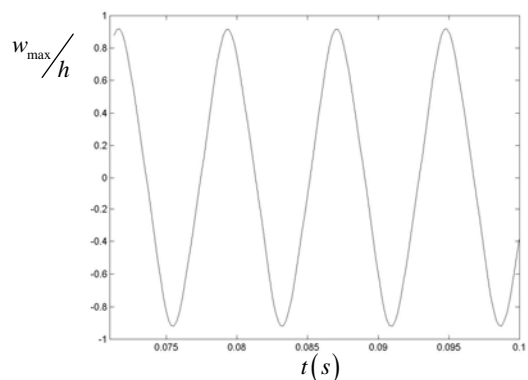


Figure 34 - Time domain response of Plate 2, (0,-0, 0, -0,0), due to harmonic excitation by a plane wave of $500 N/m^2$

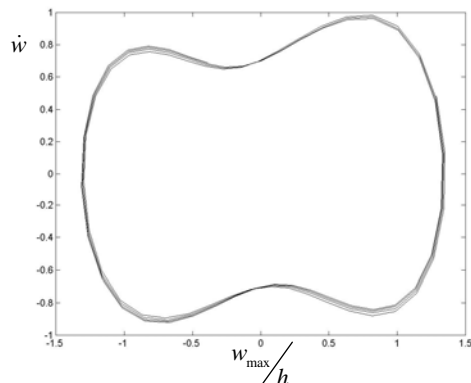


Figure 35 - Phase plane of the steady state forced vibration (1000 N/m^2) of plate 2, $(0, -0, 0, -0, 0)$, due to harmonic excitation by a plane wave

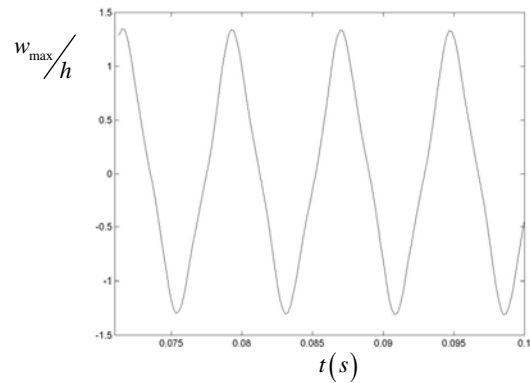


Figure 36 - Time domain response of Plate 2, $(0, -0, 0, -0, 0)$, due to harmonic excitation by a plane wave of 1000 N/m^2

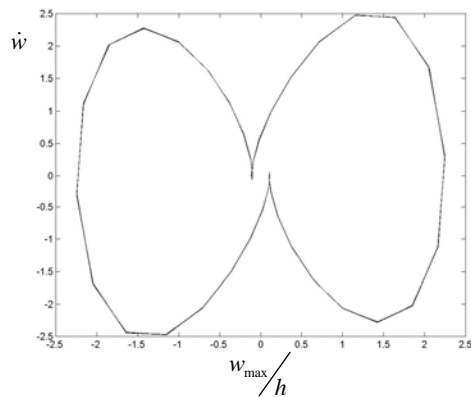


Figure 37 - Phase plane of the steady state forced vibration (2500 N/m^2) of plate 2, $(0, -0, 0, -0, 0)$, due to harmonic excitation by a plane wave

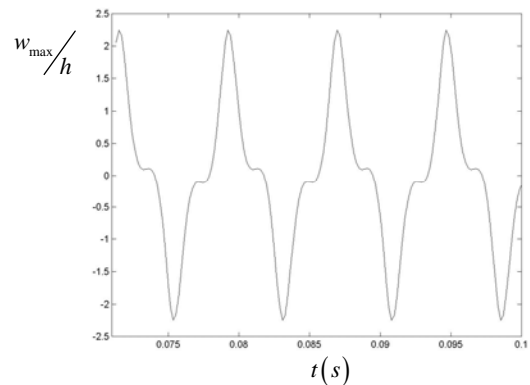


Figure 38 - Time domain response of Plate 2, $(0, -0, 0, -0, 0)$, due to harmonic excitation by a plane wave of 2500 N/m^2

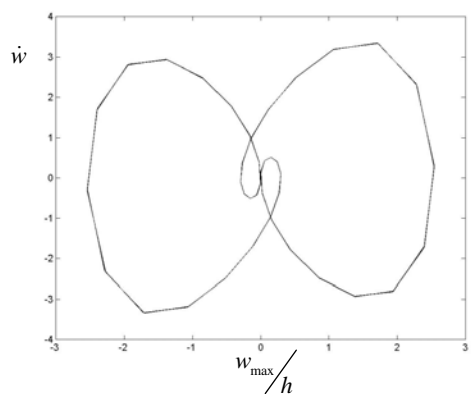


Figure 39 - Phase plane of the steady state forced vibration (3000 N/m^2) of plate 2, $(0, -0, 0, -0, 0)$, due to harmonic excitation by a plane wave

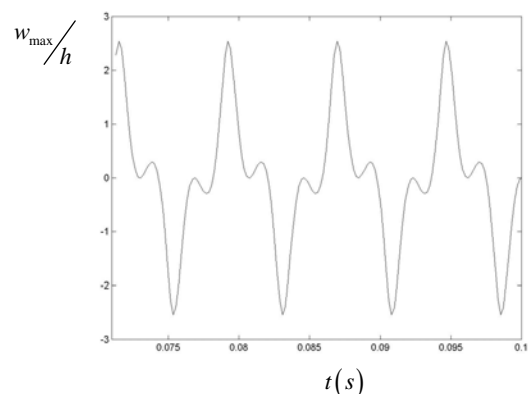


Figure 40 - Time domain response of Plate 2, $(0, -0, 0, -0, 0)$, due to harmonic excitation by a plane wave of 3000 N/m^2

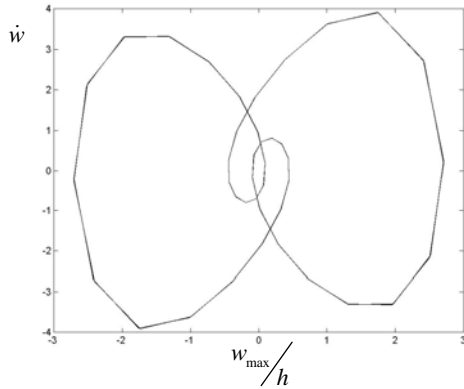


Figure 41 - Phase plane of the steady state forced vibration (3300 N/m^2) of plate 2, $(0, -0, 0, -0, 0)$, due to harmonic excitation by a plane wave

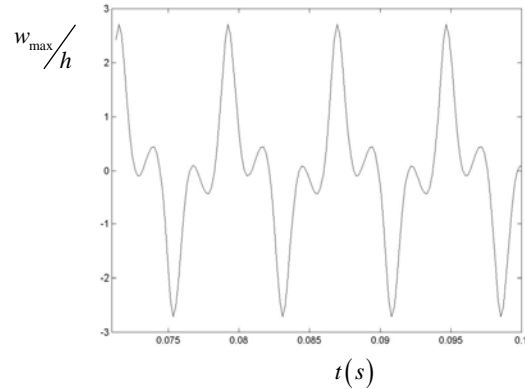


Figure 42 - Time domain response of Plate 2, $(0, -0, 0, -0, 0)$, due to harmonic excitation by a plane wave of 3300 N/m^2

Table 16 - Forced Vibration, Plate 2, $p_0=5$

P_d (N/m^2)	$P_d = 4$	$P_d = 50$	$P_d = 500$	$P_d = 1000$	$P_d = 2500$	$P_d = 3000$	$P_d = 3300$
ω / ω_{l1}	w_{\max} / h						
1.0002	0.0124	0.1524	0.9172	1.3322	2.2490	2.5414	2.7125

In

Table 16, for plate 2 and for $\theta = 0^\circ$, the value of w_{\max} / h increases as the force increases. Comparing with $\theta = 30^\circ$ and $\theta = 45^\circ$, one sees that the lower vibration amplitudes occur for this orthotropic plate.

In figures 43-48, a periodic motion is achieved for Plate 1, $(90, -45, 45, 0)_{\text{sym}}$, increasing the force applied from 5 N/m^2 to 1250 N/m^2 , and the results are given by:

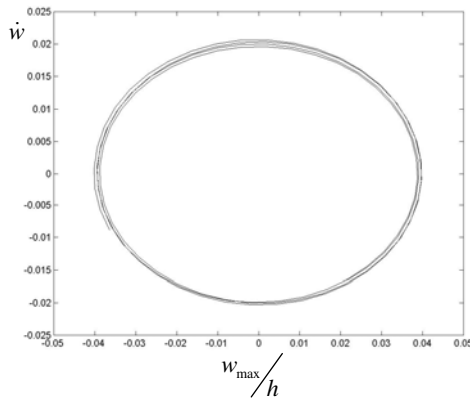


Figure 43 - Phase plane of the steady state forced vibration (5 N/m^2) of plate 1, $(90,-45, 45, 0)_{\text{sym.}}$, due to harmonic excitation by a plane wave.

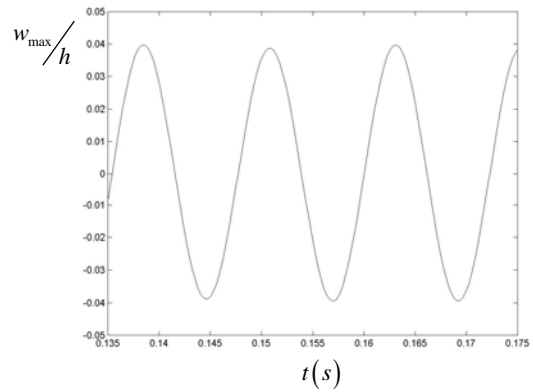


Figure 44 - Time domain response of Plate 1, $(90,-45, 45, 0)_{\text{sym.}}$, due to harmonic excitation by a plane wave of 5 N/m^2

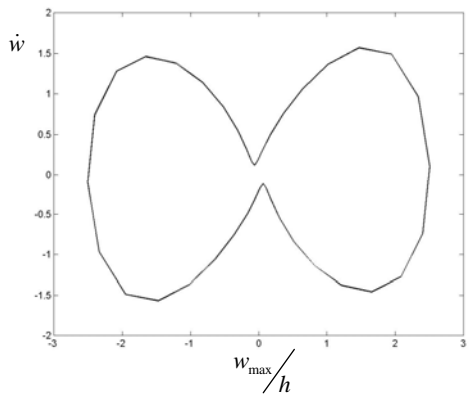


Figure 45 - Phase plane of the steady state forced vibration (1000 N/m^2) of plate 1, $(90,-45, 45, 0)_{\text{sym.}}$, due to harmonic excitation by a plane wave.

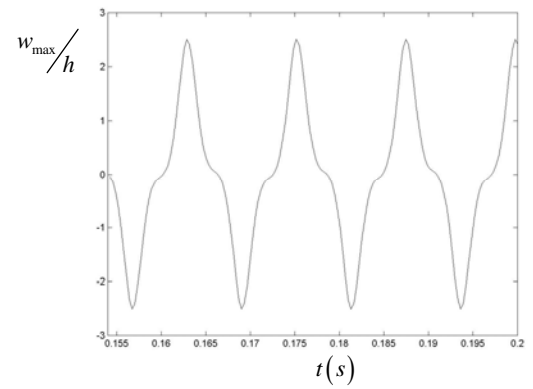


Figure 46 - Time domain response of Plate 1, $(90,-45, 45, 0)_{\text{sym.}}$, due to harmonic excitation by a plane wave of 1000 N/m^2

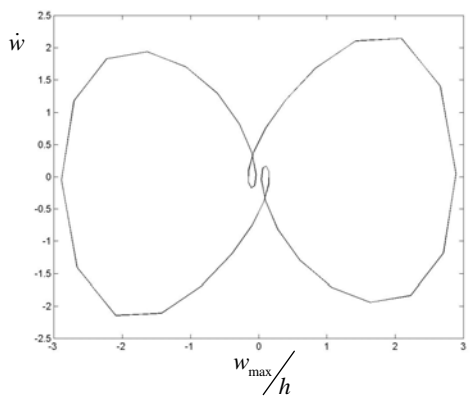


Figure 47 - Phase plane of the steady state forced vibration (1250 N/m^2) of plate 1, $(90,-45, 45, 0)_{\text{sym.}}$, due to harmonic excitation by a plane wave

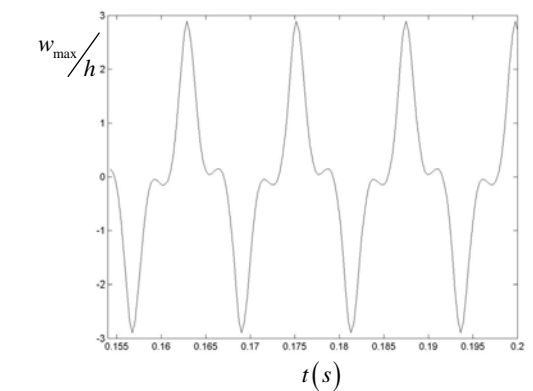


Figure 48 - Time domain response of Plate 1, $(90,-45, 45, 0)_{\text{sym.}}$, due to harmonic excitation by a plane wave of 1250 N/m^2

Table 17 shows that as the force increases, the amplitude of vibration also increases, as expected.

Table 17 - Forced Vibration, Plate 1, $p_0=5$

P_d (N/m^2)	$P_d = 5$	$P_d = 1000$	$P_d = 1250$
w/w_{11}	w_{max}/h		
1.0001	0.0397	2.5077	2.8924

Considering plate 2, with $\theta = 45^\circ$ excited by a plane wave of $4 N/m^2$, the Poincaré map is given by

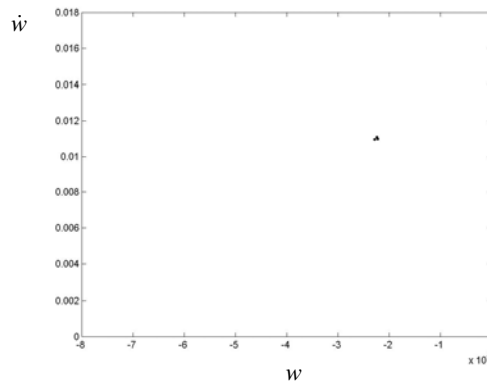


Figure 49 – Poincaré map of plate 2, $\theta = 45^\circ$ excited by a plane wave of $4 N/m^2$

The attractor is given by $(w, \dot{w}) = (-2,22E-6;1,10E-2)$. Increasing the force applied to the plate, the Poincaré maps obtained are given by

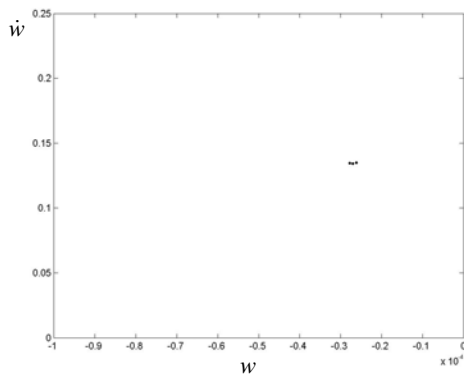


Figure 50 - Poincaré map of plate 2 $\theta = 45^\circ$ excited by a plane wave of $50 N/m^2$

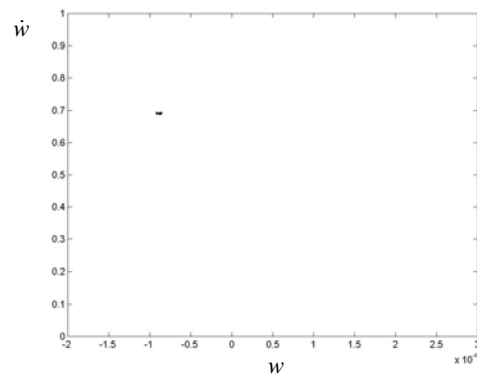


Figure 51 - Poincaré map of plate 2 $\theta = 45^\circ$ excited by a plane wave of $500 N/m^2$

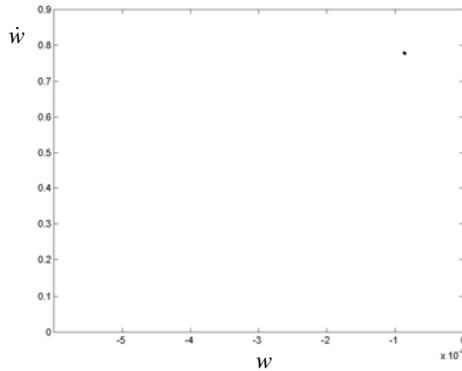


Figure 52 - Poincaré map of plate 2 $\theta = 45^\circ$ excited by a plane wave of 1000 N/m^2

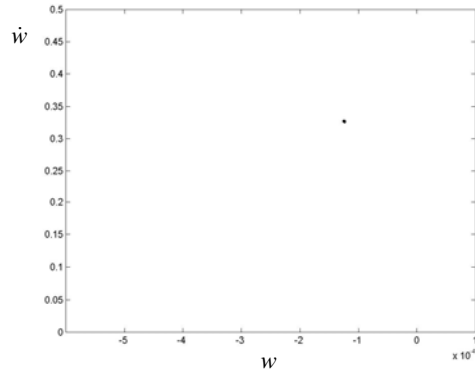


Figure 53 - Poincaré map of plate 2 $\theta = 45^\circ$ excited by a plane wave of 2000 N/m^2

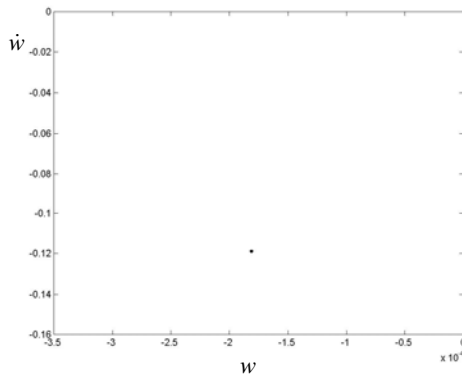


Figure 54 - Poincaré map of plate 2 $\theta = 45^\circ$ excited by a plane wave of 2500 N/m^2

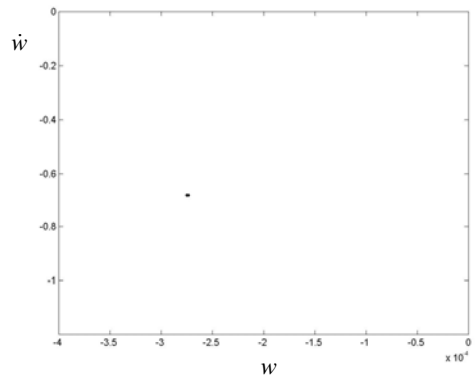


Figure 55 - Poincaré map of plate 2 $\theta = 45^\circ$ excited by a plane wave of 3000 N/m^2

From the Poincaré maps in Figures 50 – 55, a stable solution is found. The attractors obtained for a distributed force are presented in Table 18.

Table 18 – Attractor points for vibration of plate 2, $(45,-45,45,-45,45)$ with different forces applied to the plate, $\alpha = 0.0001$

Force (N/m^2)	(w, \dot{w})	
4	-0.000002221029	0.011001843
50	-0.000026992038	0.13423767
500	-0.000086438719	0.69142843
1000	-0.000086060785	0.77764522
2000	-0.00012402394	0.32740296
2500	-0.00018110176	-0.11912573
3000	-0.00027464819	-0.68290308

Considering plate 2, with $\theta = 30^\circ$ excited by a plane wave increased from 4 N/m^2 to 3000 N/m^2 the Poincaré maps are given by

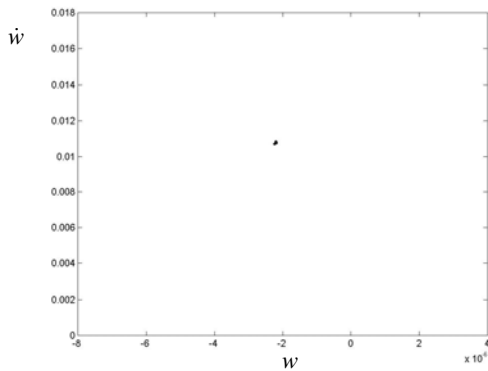


Figure 56 - Poincaré map of plate 2 $\theta = 30^\circ$ excited by a plane wave of 4 N/m^2

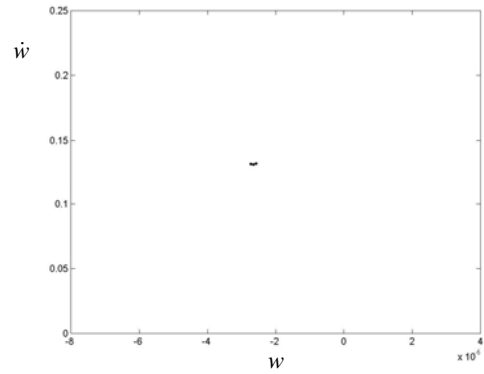


Figure 57 - Poincaré map of plate 2 $\theta = 30^\circ$ excited by a plane wave of 50 N/m^2

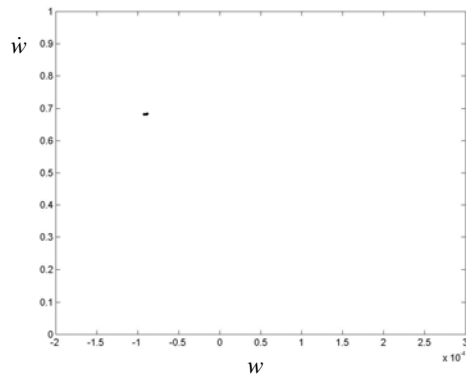


Figure 58 - Poincaré map of plate 2 $\theta = 30^\circ$ excited by a plane wave of 500 N/m^2

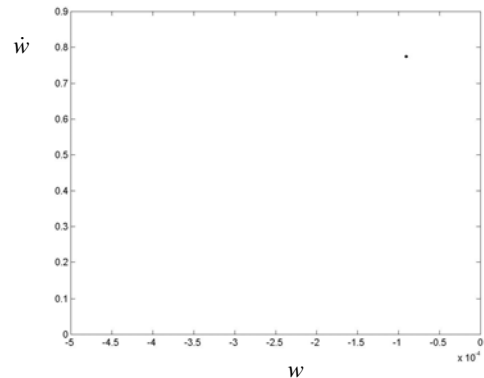


Figure 59 - Poincaré map of plate 2 $\theta = 30^\circ$ excited by a plane wave of 1000 N/m^2

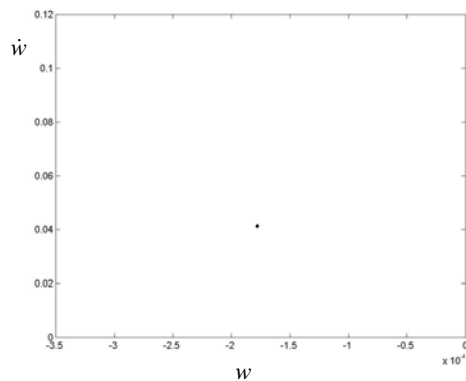


Figure 60 - Poincaré map of plate 2 $\theta = 30^\circ$ excited by a plane wave of 2500 N/m^2

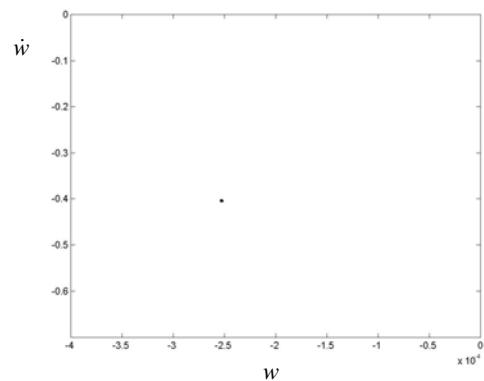


Figure 61 - Poincaré map of plate 2 $\theta = 30^\circ$ excited by a plane wave of 3000 N/m^2

From Figures 56 – 61, a stable fixed point is obtained, and the attractors are given in Table 19:

Table 19 - Attractor points for vibration of plate 2, (30,-30,30,-30,30) with different forces applied to the plate, $\alpha = 0.0001$

Force (N/m^2)	(w, \dot{w})	
4	-0,000002181	0,010768813
50	-0,000026514	0,131442280
500	-0,000088687	0,682919900
1000	-0,000090239	0,774106780
2500	-0,000177679	0,041165870
3000	-0,000253100	-0,404419910

For $\theta = 0^\circ$, a stable fixed point is also obtained for each force applied to the plate, and the attractors are given by

Table 20 - Attractor points for vibration of plate 2, (0,0,0,0,0) with different forces applied to the plate, $\alpha = 0.0001$

Force (N/m^2)	(w, \dot{w})	
4	-0,000002044	0,009946810
50	-0,000024766	0,121444390
500	-0,000085226	0,605365370
1000	-0,000118215	0,669787950
2500	-0,000105753	-0,061999104
3000	-0,000162891	-0,511205420
3300	-0,000210974	-0,800784570

For plate 1, the attractors are given in Table 21:

Table 21 - Attractor points for vibration of plate 1, with different forces applied to the plate, $\alpha = 0.0001$

Force (N/m^2)	(w, \dot{w})	
5	-0,000003785	0,019950001
1000	-0,000059534	0,121326650
1250	-0,000112039	-0,167648940

5. CONCLUSIONS

In this chapter, forced vibrations of composite laminated plates modelled by the HFEM are analysed. Linear and non-linear analyses are carried out. The linear frequencies were determined for plate 1, 2 and 3, and by comparison with numerical results, the model is validated and it is demonstrated that the linear natural frequencies of the first order shear deformation model for thick plates are lower than those from the thin plate theory, where the rotatory inertia and shear deformation are neglected. The influence of b/h was investigated, and as expected, for thin and moderately thick plates, the linear frequencies are lower than for thick plates. Therefore, the thicker the plate, the higher the linear natural frequencies predicted.

The influence of the fibres orientation is studied for plate 2 with $\theta = 0^\circ, 30^\circ$ and 45° and the linear natural frequency parameter is determined. As the angle increases, the value of the linear natural frequency parameter also increases, which indicates that the fibres orientations influence the linear natural parameter, therefore the value of the linear natural frequency.

In non-linear forced vibrations, plate 2 ($\theta = 0^\circ, 30^\circ$ and 45°), and plate 1 are studied. The force impinging on the plate's surface is increased.

Plate 1 is excited by a harmonic wave of $5 N/m^2$ to $3000 N/m^2$, at $511.112 rad/s$ and 123 DOF are considered. Plate 2 is excited by a harmonic wave of $4 N/m^2$ and 123 DOF ($p_i=7, p_o=5, p_\theta=7$) are considered in the model. The fibres orientation varies from $\theta = 0^\circ$ to $\theta = 45^\circ$. The force applied to the plate is increased to $3000 N/m^2$ for $\theta = 30^\circ$ and $\theta = 45^\circ$; for $\theta = 0^\circ$ it is increased to $3300 N/m^2$. The influence of the loss parameter is investigated and is concluded that diminishing the value of α implies an increase in the amplitude of vibration. For amplitudes of vibration of the order of the thickness of the plate, the solution was always periodic and highly dominated by the harmonic with frequency equal to the excitation frequency (principal harmonic).

In both cases, as the force increases, so does the amplitude of vibration. Periodic motions are obtained for both plates and the results are confirmed with the computation of Poincaré maps and the Fourier spectrum.